

Correlated variations in EEG pattern and visual responsiveness of cat lateral geniculate relay cells

Bing Li*, Klaus Funke, Florentin Wörgötter and Ulf T. Eysel

*Institute of Physiology, Department of Neurophysiology, Ruhr-Universität Bochum, 44780 Bochum, Germany and *Laboratory of Visual Information Processing, Institute of Biophysics, Academia Sinica, Beijing 100101, The People's Republic of China*

(Received 24 June 1998; accepted after revision 16 October 1998)

1. Simultaneous recordings of the EEG and the visual activity of cat dorsal lateral geniculate nucleus (dLGN) relay cells were analysed for covariance. Sliding time-window analyses were performed in parallel for the EEG power spectrum and single unit visual activity. The EEG power ratio (EEG-PR) of low (1–8 Hz) to high (20–40 Hz) frequencies was chosen to achieve a quantitative measure of the EEG which could be compared with the spike rate of a dLGN unit at any time. A high EEG-PR value indicates a synchronized EEG dominated by low frequencies (δ waves and sleep spindles), a low value indicates a less synchronized EEG.
2. In the anaesthetized animal, two different underlying patterns of activity in the EEG-PR were found: slow gradual changes (slow gradations) and oscillatory changes. In many cases both were accompanied by correlated variations in dLGN spike rate, either for overall activity or for burst firing.
3. The slow gradations appear for long time periods of up to 200 s and, in most cases (76.3%), show a negative correlation between EEG-PR and overall spike rate, but predominantly a positive correlation for burst firing (85.1%).
4. The oscillatory changes, which have not previously been reported, appear as temporally well-coupled variations in EEG-PR and spike rate with a stable cycle length within the range 4–10 s. In about 77% of correlated changes the temporal delay between the change in EEG-PR and that of the spike rate was less than ± 1.0 s.
5. During simultaneous recordings from two dLGN cells the variations in spike rate tend to show the same sign of correlation with respect to the EEG pattern. This relationship is more pronounced with the slow gradations than with the oscillatory changes.
6. Slow gradations in the spectral composition of the EEG may indicate global transitions between different stages within the sleep–wake cycle, reflecting the well-known influences of the brainstem arousal system. The oscillations in the spectral composition of the EEG are accompanied by gradual variations in thalamic transmission mode and are more likely to be due to involvement of a local feedback system via the thalamo-cortico-thalamic loop. The difference between the effects on overall and burst firing activity supports the notion that phasic (burst firing) and tonic visual responses may play distinctive roles in information processing, which are functionally related to the animal's behavioural state.

Electroencephalography is the most commonly used technique for monitoring the gross electrical activity of the cerebral cortex. The global states of the brain, for example different levels of sleep and wakefulness, can easily be distinguished and assessed by analysis of the spectral composition of the electroencephalogram (EEG). The preponderance of one or another frequency band is generally associated with certain behavioural states of the brain. Usually, the EEG power spectrum is dominated by high frequencies (> 20 Hz, β and γ range) during arousal and by

low frequencies (< 15 Hz, δ and sleep-spindle range) during drowsiness and sleep (for review see Lindsley & Wicke, 1974; Basar, 1980; Steriade, 1991).

The EEG displays complex, but rhythmic patterns, which are generated in the thalamus and cerebral cortex and are modulated by the ascending network system consisting of the mesopontine brainstem, hypothalamus and basal forebrain (Steriade, 1991; Steriade *et al.* 1993a). The internal state of the cortex and associated structures often undergo periodic variations. In humans, for example, the

different sleep stages (slow wave and rapid eye movement (REM)) repeat every 90 min and this rhythm seems to continue during wakefulness, leading to a waxing and waning of attentiveness (Hobson, 1989). A similar rhythm exists in cats, but shows a shorter cycle length of roughly 30 min (Lancel *et al.* 1992; Lancel, 1993). This rhythmic change in the pattern of brain activity is an active process which is probably controlled by the ascending arousal system of the brainstem (Hobson, 1989; McCormick, 1989, 1992; Steriade & McCarley, 1990; Steriade, 1991). Although the brainstem system is thought to be the generator of these variations, little is known about the contribution made by other brain areas to this process.

The changing global activity of the brain should have effects on sensory processing and motor control (Steriade, 1991; Steriade *et al.* 1993a). However, so far we have only limited knowledge about the variations in signal processing that take place at different levels of a sensory system. Ikeda & Wright (1974) found the visual responses of cortical neurons to be less tonic during synchronized EEG, and variations in alertness were found to affect predominantly the activity of cells in the output layers V and VI (Singer *et al.* 1976; Livingstone & Hubel, 1981).

Variations in the EEG state, however, are not only reflected at the cortical level but also at earlier stages of the afferent sensory pathways. For example, it has been shown that changes in EEG pattern affect the transfer ratio of visual signals from retinal ganglion cells to relay cells of the dorsal lateral geniculate nucleus (dLGN) in cat (Coenen & Vondrick, 1972). The transfer ratio was close to 100% during arousal and could drop to less than 40% during sleep or drowsiness. This observation is in agreement with the general finding that geniculate responses tend to be less vigorous than those of their retinal counterparts (Bullier & Norton, 1979; Cleland & Lee, 1985). The reduction in geniculate responsiveness is most pronounced during a synchronized EEG, when δ waves dominate. During this state the tonic visual activity elicited by maintained or slowly changing stimulus intensity is suppressed, while strong and phasic responses induced by sudden changes in contrast are little affected (Sawai *et al.* 1988; Funke & Eysel, 1992). The change in responsiveness is also accompanied by a change in the temporal pattern of spontaneous activity. During an activated EEG, which is characterized by its lower amplitude and weak power in the δ range, dLGN relay cells fire single action potentials at a low mean frequency (5–15 Hz), while they switch to rhythmic (around 1 Hz) burst discharges of high intrinsic frequency (200–500 Hz) when the EEG shows δ waves (McCarley *et al.* 1983). The synchronized state is accompanied by a hyperpolarization of the cell membrane (Llinás & Jahnsen, 1982; Hirsch *et al.* 1983; Lo *et al.* 1991; Lu *et al.* 1992), and is influenced by the brainstem arousal system (Singer, 1977; McCormick & Pape, 1990; Steriade & McCarley, 1990; McCormick, 1992; Funke *et al.* 1993). The corticofugal feedback projection to the dLGN, however, could also be involved in an EEG-

correlated modulation of thalamic processing, since removal of feedback leads to hyperpolarization of the thalamic cell (on average -9 mV; Curró Dossi *et al.* 1992) which, in many cases, forces the cell into 'burst mode'. In this way, the cortico-thalamic feedback could both reinforce brainstem influences on thalamic sensory processing and establish a more specialized control of thalamic processing possibly independent of the global brainstem influences.

Previous findings indicate that the thalamus may play an important role in generating and conveying EEG-correlated cell response characteristics to the cortex, hence influencing and amplifying the cortical EEG pattern, which in turn directly reflects the behavioural state of the individual. However, because of the lack of effective quantitative measures in earlier work, different EEG states were only qualitatively identified, and the rather general conclusions could not characterize the relationship completely. The present study was designed to analyse quantitatively in more detail the relationship between cortical EEG and the activity of the afferent thalamic relay, so as to go beyond the hitherto existing phenomenological description. We demonstrate that slow unitary variations in EEG are often accompanied by changes in dLGN responses which show a similar time course, e.g. a progressively rising power of low EEG frequencies is accompanied by a steadily declining tonic activity in the dLGN. This finding quantitatively confirms the conclusions of previous studies (Coenen & Vondrick, 1972; Livingstone & Hubel, 1981; Sawai *et al.* 1988; Funke & Eysel, 1992). In addition, we describe a novel type of correlation between thalamic firing and EEG, an oscillatory change with a cycle length of 4–10 s. It is possible that this relatively fast periodic change of the EEG status is not based on global state variations originating in the brainstem system. The time course and the often tight coupling to the thalamic activity suggest rather the involvement of cortico-thalamic feedback.

METHODS

Anaesthesia and general procedures

Experiments were carried out in fifteen adult cats of either sex (body weight 2.5–4.0 kg). Anaesthesia was induced with ketamine hydrochloride (20–25 mg kg⁻¹ i.m.; Ketanest, Parke-Davies, Germany) and xylazine (1 mg kg⁻¹ i.m.; Rompun, Bayer, Germany). The femoral artery was cannulated for continuous infusion and the trachea intubated to allow artificial ventilation. During the electrophysiological experiments anaesthesia was then maintained by artificial ventilation with N₂O–O₂ (70:30) and halothane (0.2–0.4 vol%; Fluothane, ICI-Pharma, Germany) at a rate of 10–15 cycles min⁻¹, with the cats paralysed by alcuronium chloride infusion (0.15 mg kg⁻¹ h⁻¹; Alloferin 10, Hoffmann-La Roche, Germany). The end-expiratory CO₂ was kept at about 3.8%, body temperature at 38.0 °C, and mean arterial blood pressure maintained above 90 mmHg throughout the recording sessions. Heart rate and EEG pattern were continuously monitored. The depth of anaesthesia was increased (halothane 0.8–1.0 vol%) if there was any indication of discomfort from the animal as deduced by a rise in blood pressure. The local anaesthetic xylocaine (2%;

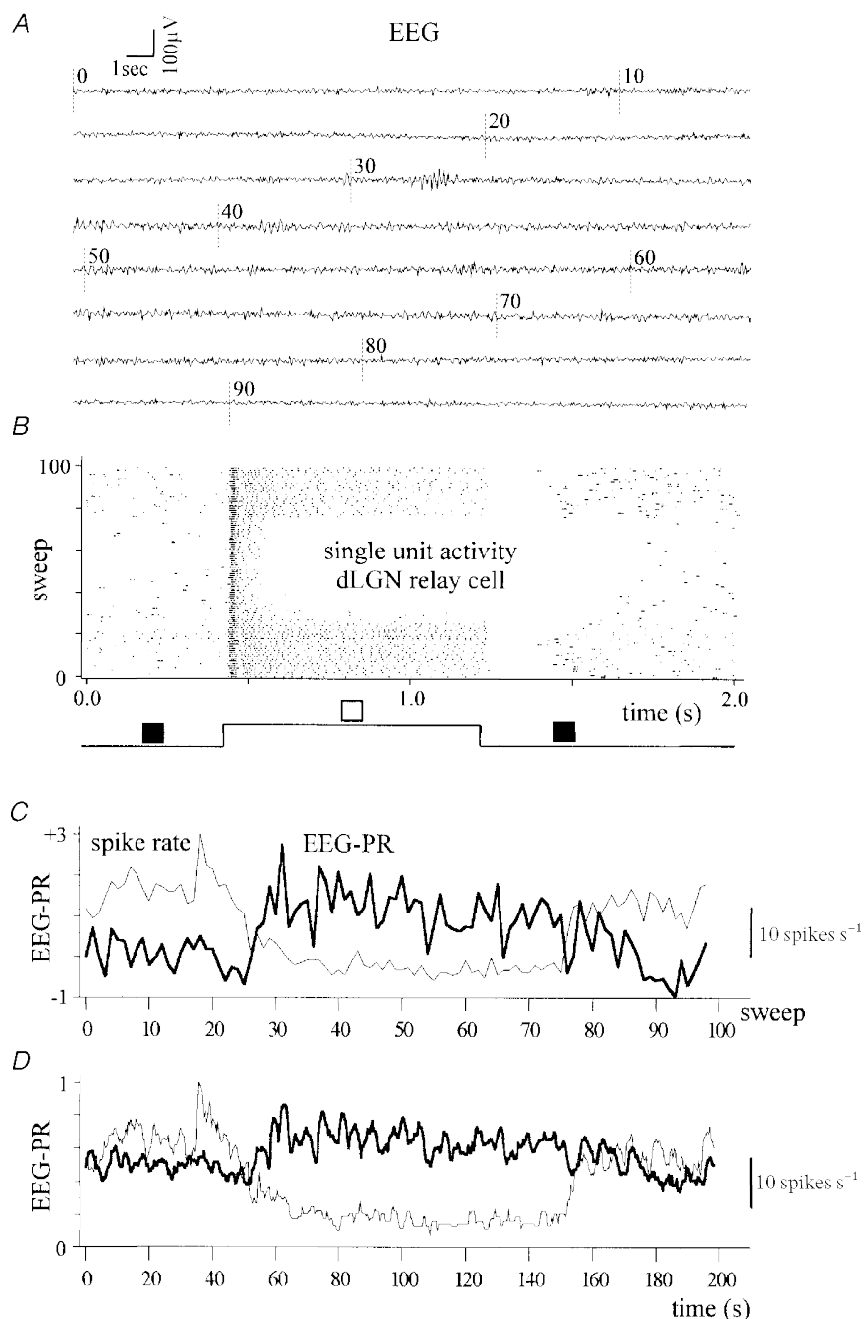


Figure 1. Original data and preliminary analysis of simultaneously recorded EEG and visual activity of a dLGN X on-cell, stimulated with a small flashing spot located in the centre of the receptive field

A, raw EEG curves plotted along the time axis. The vertical dashed lines show the time when the stimulus sweeps began every 10 trials, with the sweep numbers given above. The EEG pattern displays clear changes during the recording session, with dominating high amplitude slow waves appearing during sweeps 30–75 (more synchronized). *B*, dot raster diagram of the spike train of the dLGN cell. The ordinate depicts the sweep numbers as in *A*. The tonic part of the visual response was almost totally suppressed during the period of synchronized EEG. The stimulation protocol is given schematically at the bottom (□, spot bright; ■, spot dark). *C*, the EEG power ratio (thick line), as defined in Fig. 2, and the overall spike rate of the cell (thin line) are plotted against sweep number (analysis was performed on every real stimulus sweep instead of sliding windows). The EEG-PR curve is scaled logarithmically but without normalization. The scale bar to the right indicates the strength of neuronal activity. As judged by this plot the variations of EEG pattern and cell responses are inversely corresponding to each other. *D*, EEG-PR and spike rate are plotted against time instead of sweep number, with sliding time-window analysis applied. The EEG-PR curve has been normalized (see Methods).

Astra Chemicals, Germany) was applied to all wound margins and pressure points.

The corneae were protected with contact lenses of zero power, and accommodation to the tangent screen set at a viewing distance of 28 cm was achieved by spectacle lenses of 5–7 D selected retinoscopically (Skia-refractoscope, Heine, Germany). Atropine sulphate (1%; Atropin-Pos, Ursapharm, Germany) and phenylephrine hydrochloride (5%; Neosynephrin-Pos, Ursapharm, Germany) were applied topically for mydriasis and retraction of the nictitating membranes.

Craniotomy was performed to allow epidural EEG-registration (silver ball electrode, Brodmann areas 17/18), lowering of two concentric bipolar stimulation electrodes bilateral to the optic chiasm, and vertical access to the dorsal lateral geniculate nucleus (Horsley–Clarke co-ordinates, A3–A10, L6–L13). At the end of the experiment the cats were deeply anaesthetized (4% halothane) and perfused for histological purposes.

Recordings, visual stimulation and data collection

Extracellular recordings of action potentials of single dLGN relay cells were made with glass micropipettes broken to an outer tip diameter of 3–6 μm and filled with 3 M NaCl solution. In eight experiments, double-site recordings (simultaneous recordings from two dLGN cells) were made with two pipettes placed 300–800 μm apart from each other to check for correlated changes in neuronal activities. In double-site recordings, the receptive fields of the two cells were well separated from each other, often as far as 10 deg. Thus, it was unlikely that they shared common retinal inputs which might lead to correlated firing between nearby dLGN cells. The EEG was recorded via a silver ball electrode placed above the dura mater at the border between areas 17 and 18 of the same hemisphere, representing the central part of the visual field (up to 15 deg eccentricity), which topographically corresponded to the thalamic recording sites.

Visual stimuli were generated by a Picasso cathode ray image generator (Innisfree, Cambridge, USA) and presented on an oscilloscope screen (model 608, Tektronics, USA; frame rate, 200 Hz) 28 cm in front of the cat's eyes. Different kinds of stimuli were used, but in most cases, receptive field centre or centre-surround responses of dLGN cells were elicited using flashing spots of variable diameter (0.2–5 deg) and contrast. Flashing or moving bars, or gratings were also used in some cases. The basic settings were as follows: for the on-cells, light stimuli (intensity, 10.0–20.0 cd m^{-2}) were flashed either on a dark (0.1 cd m^{-2}) or intermediate (2.0 cd m^{-2}) background; for the off-cells, either similar stimuli were switched off to background level, or dark stimuli (0.1 cd m^{-2}) were presented on the intermediate background illumination. Background room illumination was kept at about 1 cd m^{-2} . Each stimulus cycle was composed of 400 ms stimulus off, 800 ms on and finally 800 ms off, i.e. every sweep had a duration of 2000 ms.

Amplified analog single unit action potentials were selected through a window-discriminator (model 121, World Precision Instruments, USA), converted to TTL-pulses and fed on-line via a laboratory interface (model 1401, Cambridge Electronic Design, UK) into a personal computer. Sweep onset and spike firing times were stored on disk with a temporal resolution of 125 μs . Usually each recording contained about 100 sweeps of identical stimulus presentation. In parallel to the single unit activity, the EEG was continuously recorded by analog amplification with a gain of 10 000 or 20 000 and, following digitalization, via an A/D-converter at a sampling frequency of 250 Hz.

Classification of the cells

The geniculate relay cell types X, Y, on and off were identified by visually testing the spatio-temporal characteristics of their receptive fields (Derrington & Fuchs, 1979). In a few experiments, the response latency to electrical stimulation of the optic chiasm was also taken into account (Y cells, 1.1–1.5 ms; X cells, 1.6–2.2 ms; Stone & Hoffmann, 1971). Ultimately, however, the results from all cells were pooled because, so far as the properties examined are concerned, we found no significant difference between cells of the different types.

Data analysis

In the present and previous studies (Funke & Eysel, 1992), we found that the most remarkable changes in dLGN activity predominantly occurred with variations in the amount of δ (0.5–3.5 Hz) and θ (4–7 Hz) waves in EEG (also see Sawai *et al.* 1988). An increase in the slow wave activity was frequently accompanied by a decline in geniculate responsiveness. Although such a dramatic 'wax and wane' is unlikely to be accomplished within a period as short as our recording episodes (normally about 200 s), Fig. 1 gives a distinctive example showing the close relationship between slow wave activity and geniculate response strength. An increase in the power in the low-frequency range (predominantly the range of δ and θ waves and sleep spindles) usually is coupled with a decrease in power in the high-frequency range (β and γ) and vice versa. For convenience in quantitatively describing the spectral composition of the EEG with a single parameter we calculated the 'EEG power ratio' (EEG-PR), as the ratio of the power of low (1–8 Hz) to high (20–40 Hz) frequencies. This ratio was found to be the most sensitive measure for changes in the spectral composition of the EEG (see Fig. 1C and D). A sliding time-window technique was utilized to give an almost continuous display of the spectral composition of EEG at very short time intervals. Figure 2 gives a schematic illustration of the sliding time-window analysis. Fast Fourier transformation (FFT) was applied to a window of 2048 ms, which roughly corresponds to one complete stimulus cycle (2000 ms), and the window was shifted in steps of 100 ms for every new calculation. This sliding time-window technique was used for two reasons: (i) with the sliding window we can achieve an enhanced temporal resolution of 100 ms compared with 2.0 s if the analysis were applied to complete stimulus sweeps; (ii) because of this higher temporal resolution, we can obtain a near 20-fold larger number of data points for the EEG-PR and the firing rate, which leads to a much more efficient and precise cross-correlation between EEG-PR and spike rate curves, especially in the case of fast (oscillatory) changes (see below).

The following steps were performed to obtain the EEG-PR value from each time window (see Fig. 2A): (i) FFT-analysis of the original EEG curve within the window of 2048 ms; (ii) summation of the power spectrum in the frequency ranges 1–8 Hz (P_L) and 20–40 Hz (P_H), respectively; (iii) calculation of the EEG-PR of the low-frequency range divided by the high-frequency range, then transformed logarithmically to balance the general amplitude differences of the low and high-frequency components ($\text{EEG-PR} = \log_{10}(P_L/P_H)$). The neuronal responsiveness of dLGN cells was determined as the count of all spikes occurring in roughly the same time window (2000 ms, has to be one complete stimulus-response sequence in the case of sliding time window) and converted into spike rate (spikes s^{-1}). In addition to the calculation of the overall spike rate within the sliding time window, the rate of burst firing and the contribution of different response components (phasic and tonic responses and spontaneous activity) were also analysed. By plotting all the EEG-PR and spike rate values obtained from one recording *versus* time, we obtained the

curves for corresponding changes in EEG pattern and neuronal response strength with a temporal resolution of 0.1 s. The EEG-PR curves were finally normalized with reference to the minimal and maximal values obtained within the same experiment to compensate for any differences resulting from different experimental settings. Thus, 0 represents an activated EEG with the lowest δ power in a given experiment and 1 the most synchronized EEG with the highest δ power. The [0,1] scale will be applied to all EEG-PR curves in the figures throughout this paper.

Variations in EEG-PR and spike rate appeared with very different time courses and therefore could not be analysed with one standard procedure. For the slow and steady changes (slow gradations) in

EEG-PR and spike rate which could span the duration of a whole recording or longer we chose linear regression analysis; for the faster (oscillatory) changes, the cross-correlation function (CCF) was chosen. Prior to these processes all curves were smoothed to remove noise, artefacts, and low- or high-frequency components. Alternative filter settings (see Fig. 2*B*) were designed to emphasize the different temporal aspects of variations in EEG-PR and spike rate curves as described below. Figure 3 gives an example for the results of these filtering processes. At this point it is important to note that the frequencies mentioned here refer to the temporal characteristic of the EEG-PR which resembles the changes in the spectral composition of the EEG over time and not to the frequencies contained in the original EEG signal.

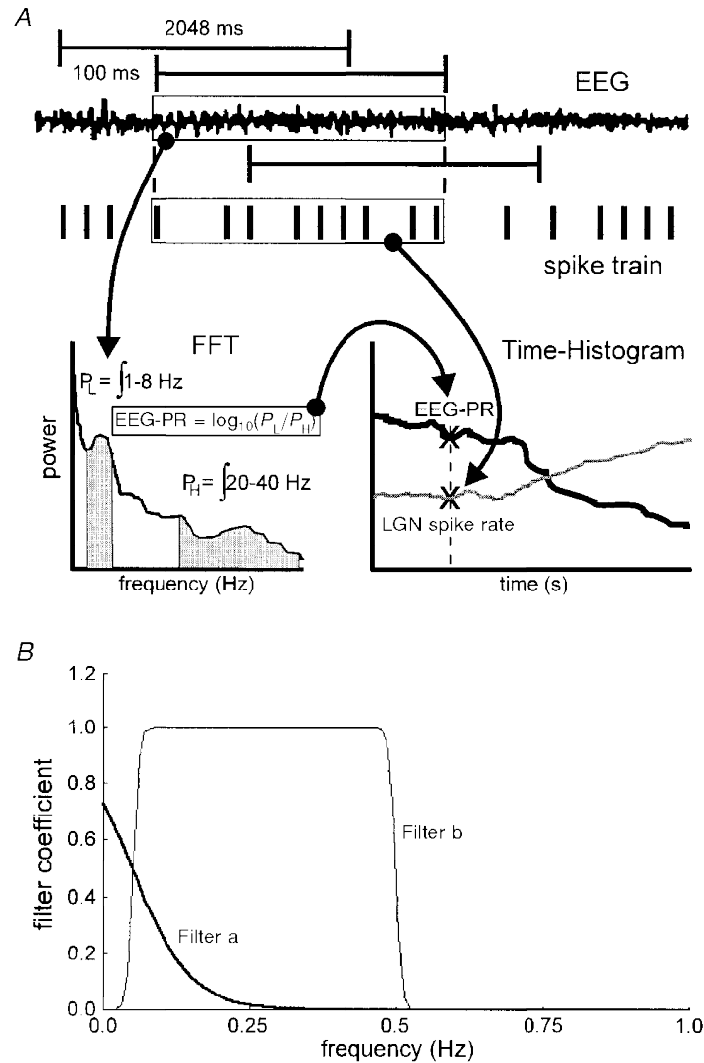


Figure 2. Schematic illustration of the sliding time-window analysis of EEG and simultaneously recorded dLGN spike activity

A, in a time window of 2048 ms (as indicated by horizontal bars), almost equally sized to stimulus sweep length (~2000 ms), the power spectrum of the EEG was determined by FFT. In parallel, the mean spike rate of the neuron (boxed portion of the spike train) was determined in a window of 2000 ms (corresponding to the sweep length). Spike rate and the logarithm of the ratio of the summed-power of low (1–8 Hz) vs. high (20–40 Hz) EEG-frequency bands ($\text{EEG-PR} = \log_{10}(\sum \text{power}_{1-8 \text{ Hz}} / \sum \text{power}_{20-40 \text{ Hz}})$) were then plotted along the time axis at the starting point of the time window (crosses). The complete curves are obtained by repeating this procedure for consecutive time windows, shifted in steps of 100 ms. *B*, diagram showing the characteristics of the two temporal filters used to emphasize either the components of the slow (filter a) or the fast (filter b) events.

Slow gradations. To specify the slow variations in the spectral composition of the EEG (EEG-PR) and spike rate, called 'slow gradations', we preserved the linear trend and the low-frequency components of both EEG-PR and spike rate curves, but removed the higher frequencies as follows: (i) the curve was smoothed with a low-pass filter (Fig. 2B, filter a), the cut-off frequency was 0.05 Hz; (ii) linear regression was then performed on both curves, calculating K_p as the slope of the EEG-PR curve and K_s as the slope of the spike rate curve. The sign (plus or minus) of their product ($K_p \times K_s$)

gave the correspondence (positive or negative correlation) between the two measures.

Oscillations. For the purpose of the CCF-analysis to check for the relatively fast correlated changes occurring periodically in the EEG-PR and the spike rate (oscillations), the following procedures were carried out on both curves (for mathematical reference see Press *et al.* 1988). (i) The linear trend was removed by subtracting a straight line which intercepted the first and last data points of the curve. (ii) The curve was then smoothed with a band-pass filter

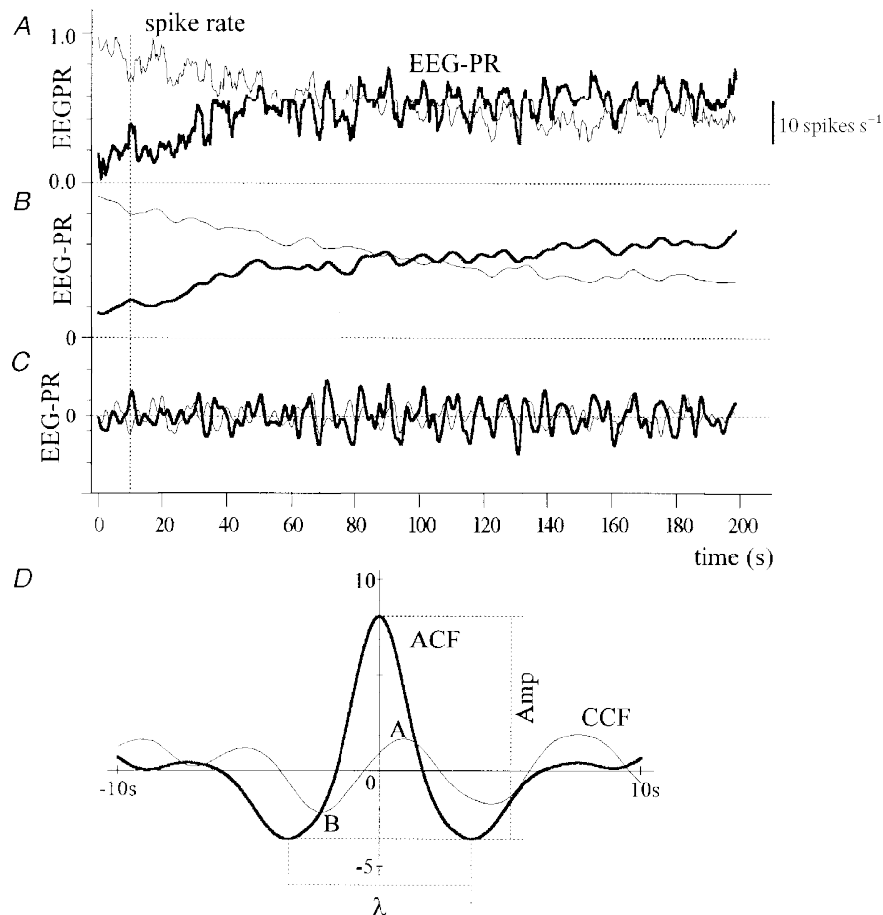


Figure 3. Examples of EEG-PR and spike rate curves (for a Y on-cell) illustrating the analysis procedure using the different filter settings and the calculation of the auto- and cross-correlation functions (ACF and CCF, respectively)

Here and in subsequent figures EEG-PR and spike rate curves are shown as thick and thin lines, respectively. The scale bar to the right indicates the strength of cell activity. Thin lines are also used for cross-correlograms, shown at 1000-fold the original amplitude. The dashed vertical lines indicate the CCF window. *A*, raw curves without smoothing. It can be seen that fast fluctuations occur simultaneously with slow graded variations of both curves. *B*, curves smoothed with filter a (see Fig. 2B) to eliminate the fast (oscillatory) changes, thereby allowing the slow changes to be seen. The EEG-PR curve shows a steady increase ($K_p = 1.995 \times 10^{-3} \text{ s}^{-1}$), which is accompanied by a clear decrease in the spike rate curve ($K_s = -4.671 \times 10^{-3} \text{ spikes s}^{-1}$), an example of negatively correlated slow gradations. *C*, curves smoothed with filter b to display only the oscillatory events. Since the DC component has been totally removed, the curves fluctuate around the zero level (dashed horizontal line in the middle). The temporal relationship between the two signals is much better visible in *D*, with CCF. *D*, the CCF (thin line) of the two curves shown in *C*, is characterized by an amplitude of 3.603×10^{-3} , a temporal offset of 0.9 s for point A with respect to the origin and a wavelength (λ) of 6.5 s, indicating positively correlated oscillatory events. The value for temporal shift of CCF is in this case determined by the offset of point A, since this is the extremum point closest to the ordinate axis. The ACF of EEG-PR curve is shown by the thick line (Amp = 11.66×10^{-3} ; λ , 7.0 s). Measurement of Amp and λ is illustrated in the ACF correlogram.

Table 1. Statistics for slow gradations of the EEG power ratio (EEG-PR) and the overall spike rate

$ K_p $ (10^{-3} s^{-1})	Total no. recordings	No. positive correlations	No. negative correlations	$ K_s $ (10^{-3} spikes s^{-1})
0.0–0.4	2017	891 (44.2%)	1126 (55.8%)	1.773
0.4–0.8	743	302 (40.6%)	441 (59.4%)	2.115
0.8–1.2	313	111 (35.5%)	202 (64.5%)	2.496
1.2–1.6	102	26 (25.5%)	76 (74.5%)	3.430
Above 1.6	35	8 (22.9%)	27 (77.1%)	4.149
Total	3210	1338 (41.7%)	1872 (58.3%)	2.001
Above 0.8	450	145 (32.2%)	305 (67.8%)	2.837

All 3210 recordings of spike activity had a mean spike rate above $10.0 \text{ spikes s}^{-1}$. No threshold was set for K_p or K_s . Samples are subdivided into five categories, according to the absolute values for the slope of the EEG-PR curve ($|K_p|$), as obtained from linear regression analysis. For each category, the total number, the number and percentage (in parentheses) of positive and negative correlations, and the mean absolute slope of the spike rate curve ($|K_s|$) are listed in the corresponding columns. The two last rows give the results for the total sample and for the sample with $|K_p| > 0.8 \times 10^{-3} \text{ s}^{-1}$, which was the threshold set to identify significant cases for EEG-PR slow gradations. Note that both the mean value of $|K_s|$ and the percentage of negative correlations increase with $|K_p|$.

(Fig. 2*B*, filter *b*). The cut-off frequencies were 0.05 and 0.5 Hz at the low and high ends, respectively, so that the highest frequency components were also removed together with possible noise and artefacts. (iii) CCF was calculated between EEG-PR and spike rate curves within a time window of -10.0 to $+10.0$ s. The resulting correlogram was normalized by the length of the CCF window (between the two vertical dashed lines in Fig. 3*A–C*) to correct for the different durations of the whole recordings. (iv) The normalized correlogram was then used to determine the correlation strength (amplitude), the wavelength (oscillatory period, λ) and the temporal shift (see Fig. 3*D*). The polarity (positive or negative) of the correlation between the two curves is given by the sign of the correlation amplitude (Amp).

To check for oscillatory changes in the EEG-PR *per se*, the auto-correlation function (ACF) was chosen and similar procedures were applied to the EEG-PR curves.

Threshold settings. In this study we analyse the correlation of two different electrical signals (spike trains and EEG) which are both affected by electromagnetic noise. *A priori*, we cannot be sure that our analysis detects only real systemic signal variations and not those that are intrinsic to the electromagnetic noise. In order to achieve an estimate of the contribution of fluctuations due to noise in the correlation between EEG-PR and spike rate variations, we ran a series of simulated control tests to determine appropriate thresholds. Two random noise sequences which also include the frequencies of the original signals were produced stochastically for a period of 200 s (the usual recording time), one resulting in simulation of the EEG-PR and the other reflecting changes in spike rate. The simulated EEG-PR sequence could vary by 0.5, i.e. 50% of the possible range [0,1]; the simulated spike rate sequence could also vary by 50% of the range of experimental data. Thereafter, the two signal sequences were subjected to exactly the same analysis procedures as described above and the parameters (Amp, K_p , K_s , and so on) were calculated. This simulated control test was run repeatedly to obtain a large sample pool. We used 3000 repetitions, which is close to the size of our actual data sample. Finally, the maximum values of these parameters were taken as a basis for the thresholds in the analysis of the experimental data.

We set the thresholds as 2.5×10^{-3} for |Amp|, $0.8 \times 10^{-3} \text{ s}^{-1}$ for $|K_p|$, and $2.5 \times 10^{-3} \text{ spikes s}^{-1}$ for $|K_s|$, which are reasonable values close to the individual maxima and were surpassed by only a few samples (less than 0.3%) in the simulated pool.

Burst activity. The corresponding spike rate values for burst activity were calculated as follows: (i) discrimination of the bursts in the time window (a burst episode is preceded by a silent period ≥ 50 ms and consists of at least two action potentials with interspike intervals ≤ 4 ms; see Guido & Weyand, 1995); (ii) counting the number of bursts; (iii) using the rate of burst firing instead of the mean spike rate for cross-correlation and regression analysis. Thresholds for significant changes in burst firing were corrected according to the lower mean rate of burst firing ($0.5 \text{ bursts s}^{-1}$) compared with the mean of overall firing rate (10 spikes s^{-1}).

Separate analyses for spontaneous activity, phasic and tonic responses. For recordings which showed significantly correlated variations, the same analyses were extended with the overall spike rate replaced by the spontaneous activity (in the first 400 ms of every sweep when the stimulus had not been present, and eventually the last 400 ms of the stimulus-off episode), the phasic response (about the first 100 ms of the elicited response, with an obvious peak inside), and the tonic response (the last 600 ms of the stimulus-on episode), respectively.

RESULTS

General view

Altogether, a total of 3418 pairs of data sets for EEG and spike trains obtained from 379 dLGN relay cells were analysed. Of these, 2194 sets were obtained by simultaneous recordings of two dLGN cells (1097 double-site recordings), the remaining 1224 sets were single dLGN EEG recordings. The duration of any data set was never less than 60 s (30 sweeps) and most lasted about 200 s (100 sweeps). The EEG patterns were similar to those described previously for cats

under the same type of anaesthesia (Ikeda & Wright, 1974; Funke & Eysel, 1992), and the changes in the power of δ waves were similar to those found in the behaving cat (Lancel *et al.* 1992; Lancel, 1993) but with a less pronounced activity in the high-frequency range (above 15 Hz). In a majority of the dLGN relay cells recorded, the cell type (X, Y, on or off) could be determined, but for the results described here all data sets were pooled because we did not find any significant difference between cell types.

Variations in the spectral composition of the EEG (the ratio of the power of low to high frequencies of the EEG, EEG-PR) could generally be assigned to two different categories: (i) slow gradations which appeared as unitary, steady changes

of EEG-PR and spike rate and, (ii) oscillations of both signals with a cycle length of 4–10 s. In most cases, the slow gradations were characterized by a relatively slow but steady rise or fall of the signal during the whole or much of the recording period (Figs 3 and 4A). Occasionally, the curve showed dramatic changes within a short time, e.g. a fast rise or fall with a large amplitude (Fig. 4D). In the case of the oscillatory changes most, if not all, EEG-PR curves consisted of series of regular fluctuations (oscillations), usually with cycle periods of 4–10 s (Figs 3, 6A and 8). Simultaneously, in either category, the geniculate neuronal responses also showed these kinds of changes and the spike rate curves varied either in the same or in the opposite direction with almost the same dynamics as the EEG-PR curve. Here we

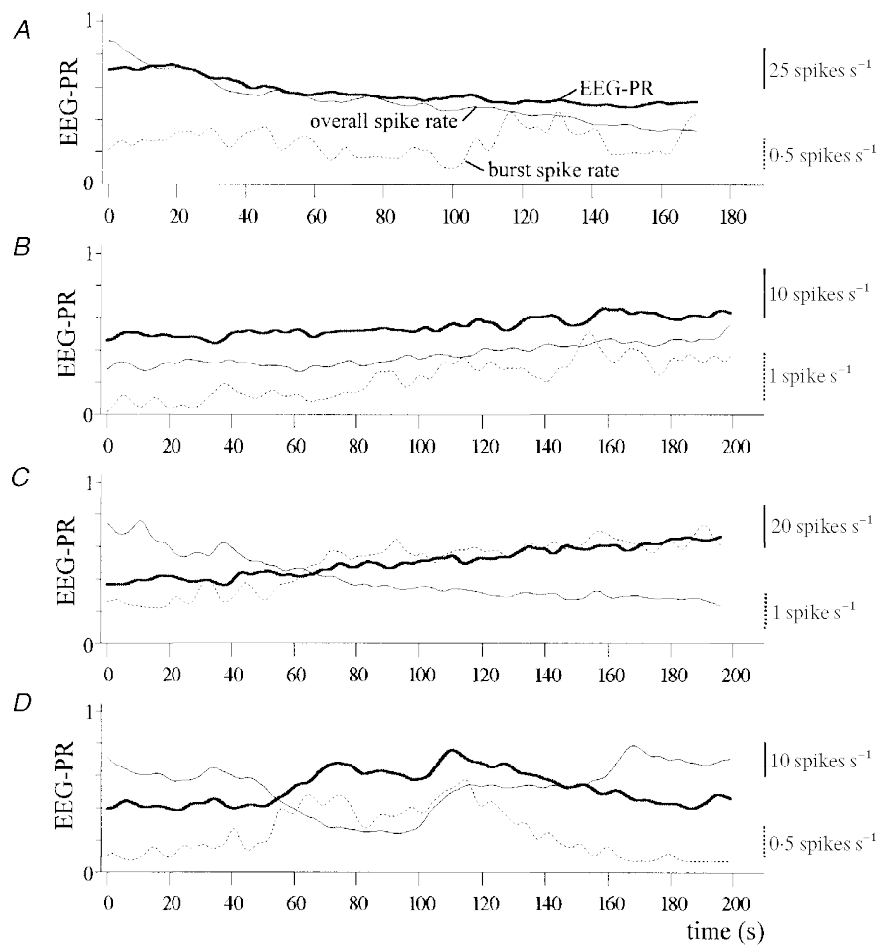


Figure 4. Examples of slow gradations in EEG-PR and spike rate

In each panel, the overall activity and burst activity of the same cell are shown with thin continuous and dashed lines, respectively, along with the corresponding EEG-PR curve (thick continuous line). All curves have been smoothed with filter a (Fig. 2). *A*, overall activity displays a positively correlated gradation in relation to the EEG pattern ($K_p = -1.420 \times 10^{-3} \text{ s}^{-1}$; $K_s = -4.937 \times 10^{-3} \text{ spikes s}^{-1}$). The weak burst firing does not show any clear gradual change. *B*, the slow variations of both, overall activity and burst activity are positively correlated to the EEG-PR. $K_p = 0.878 \times 10^{-3} \text{ s}^{-1}$ and $K_s = 2.816 \times 10^{-3} \text{ spikes s}^{-1}$ for overall activity; $K_s = 8.026 \times 10^{-3} \text{ spikes s}^{-1}$ for burst firing. *C*, the slow events are negatively correlated to the EEG for overall activity ($K_p = 1.528 \times 10^{-3}$; $K_s = -5.446 \times 10^{-3} \text{ spikes s}^{-1}$), but positively correlated for burst firing ($K_s = 4.752 \times 10^{-3} \text{ spikes s}^{-1}$). *D*, example showing several fast graded variations restricted to a shorter episode, especially visible between 40–80 s and 95–115 s. Note that the burst firing varied almost opposite to the overall activity in most parts of the recording.

will demonstrate in more detail the various correlated variations between dLGN responsiveness and EEG pattern.

Slow gradations

Slow gradations appear as unitary, steady changes, with the curves rising or falling slowly but steadily. Such events cover at least a substantial proportion of or the whole recording (200 s) and sometimes exceed 10 min, spanning several consecutive recordings. Since it is almost impossible to define the start and/or end points of such variations, we analysed only whether EEG-PR and spike rate significantly rose or fell within the same temporal interval, but did not look for the precise relationship between the two signals.

The statistics for the slow gradations in EEG-PR and spike rate are shown in Table 1 with the results obtained from overall spike rate analysis. The distribution for positively and negatively correlated cases and the mean absolute values of the slope of the spike rate curve ($|K_s|$) are given in relation to different categories of absolute slope of the EEG-PR curve ($|K_p|$). In general, the relative number of negatively correlated cases increases for stronger variations in EEG-PR (larger $|K_p|$ values). Actually, it was evident from many recordings that a very slow change in EEG-PR could be associated with a positively correlated very slow change in spike rate (see Fig. 4*A* and *B*). However, in these cases the increase in burst firing (dashed lines in Fig. 4*B*) seemed to dominate the change in overall activity. If the change in EEG-PR was stronger, the spike rate often showed a

negative correlation (Fig. 3*B* and 4*C*) and, often, a sudden increase in the slope of the EEG-PR caused a switch from a positive to a negative correlation during the recording period (for example see Fig. 7*D*). The bottom row of Table 1 shows the number of cases (450) with $|K_p|$ larger than $0.8 \times 10^{-3} \text{ s}^{-1}$, which we then also used as the threshold setting for further analysis of significant changes in EEG-PR. This quite small fraction of 14% (450/3210) indicates that strong changes in the spectral composition of the EEG did not occur very often in the almost continuous series of EEG and spike recordings and were interspersed with longer periods of stable EEG conditions (see discussion related to sleep stages). Of these cases, 186 (41.3%) events showed a change in overall spike rate larger than the reference threshold ($|K_s| > 2.5 \times 10^{-3} \text{ spikes s}^{-1}$). In this sample of 450 strong changes a negative correlation between the EEG-PR and the spike rate was significantly more frequent than in the overall sample (one row above, $P < 0.001$).

Dorsal lateral geniculate nucleus relay cells can show two different patterns of activity: burst discharges (usually 2–7 spikes at intervals less than 5 ms) and single spikes at rates of roughly 10 Hz during spontaneous activity and up to 100 Hz during visually driven, tonic activity. Bursts are the prevailing spontaneous activity pattern when the cell membrane is hyperpolarized ($< -65 \text{ mV}$), but could also contribute to visually driven activity. Following a period missing action potentials, which is often found when the cell

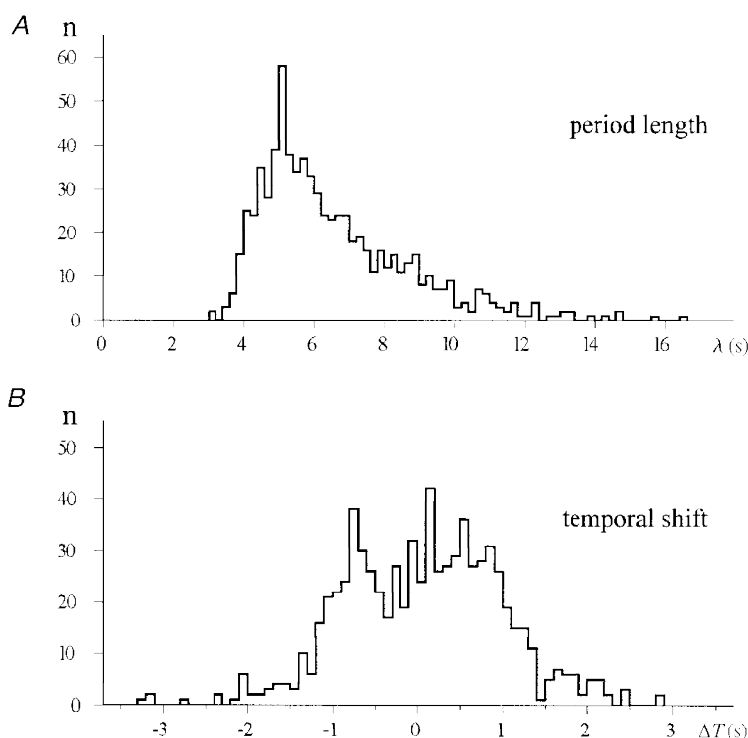


Figure 5. Distribution of the parameters for the oscillatory events

Only the significant cases ($|\Delta \text{amp}| > 2.5 \times 10^{-3}$) are included ($n = 741$). *A*, wavelength (cycle period), *B*, temporal shift.

Table 2. Statistics for oscillatory changes in the EEG-PR and the overall spike rate, no threshold setting

[Amp] (10^{-3})	Total no. recordings	No. positive correlations	No. negative correlations	Wavelength (s)
0.0–2.0	2144	1064 (49.6%)	1080 (50.4%)	4.950
2.0–4.0	824	419 (50.8%)	405 (49.2%)	6.101
4.0–6.0	150	70 (46.7%)	80 (53.3%)	6.767
Above 6.0	92	39 (42.4%)	53 (57.6%)	7.538
Total	3210	1592 (49.6%)	1618 (50.4%)	5.404
Above 2.5	741	367 (49.5%)	374 (50.5%)	6.492

Samples are subdivided into four categories, according to their absolute values for the normalized amplitude of the cross-correlation between EEG-PR and spike rate curves ([Amp]). For each category, the total number, the number and percentage of positive and negative correlations, and the mean value of the oscillation period (wavelength) are listed in the corresponding columns. The last two rows give the results for the total sample and the sample with $[\text{Amp}] > 2.5 \times 10^{-3}$ (the threshold set by the simulation study to identify significantly correlated cases). Note that the mean value of wavelength increases with [Amp].

is hyperpolarized, a sudden change in brightness of excitatory polarity can elicit a burst at the onset of the light response. Thereafter, the cell usually switches to tonic firing during maintained contrast (Lo *et al.* 1991; Lu *et al.* 1992). With a highly synchronized EEG the tonic response may be largely suppressed so that only the burst at the response onset survives (Sawai *et al.* 1988; Funke & Eysel, 1992). In a separate analysis we therefore determined also the relation of burst activity to EEG which was different from that of the overall activity. Burst firing appeared to have a larger number of significantly correlated changes (52.4% (+ and –) *vs.* 41.3% for overall activity, $P < 0.005$), although the sample size for analysing burst activity was much smaller because the contribution of bursts to overall activity was often too weak. However, the most striking difference comes from the cases showing positively correlated variations. While the analysis of overall activity yielded less than one-quarter (23.7%) of such cases, burst firing was overwhelmingly dominated by positive correlations (85.1%). Several examples which allow a comparison between the variations of overall and burst activity are shown in Fig. 4. In general, mean burst spike rate showed stronger fluctuations, in many cases showing variations opposite to the overall response (Fig. 4C and D). In total there were 78 recordings in which significant slow gradations correlated to EEG-PR could be identified in both overall and burst activities. Of these, 64 cases (82.1%) showed opposite trends in the changes of overall and burst spike rate.

Besides the long-lasting unitary gradations described above, sometimes rapid single transitions between low and high EEG-PR values occurred, usually within a shorter temporal interval of 10–50 s and also accompanied by a change in dLGN spike rate. A typical example is shown in Fig. 4D. Since the dynamics of these changes (duration, slope and temporal delay between the two signals) could vary considerably from event to event, they could not be

quantified with the simple linear regression used for slow gradations, or with other standard methods. In order to make some general statistics we modified the analytical procedure for the general slow gradations by calculating linear regressions on a series of sliding time windows. With this technique we distinguished 58 pairs of EEG-PR and overall response curve segments which displayed fast gradual changes. Of these, 51 pairs were negatively correlated, and only 7 pairs showed a positive correlation. The percentage of positive correlations (12.1%) was significantly lower than that of the general slow gradations (23.7%, $P < 0.05$). Also in this case, burst firing predominantly appeared to show a positive correlation to the EEG-PR (98/116, 84.5%), which is similar to the situation of general slow gradations (85.1%).

Since these faster changes are associated with a shorter time course and a steeper slope we could approximate the temporal delay between the variations of EEG-PR and spike rate. Statistics show that in most cases the changes in the overall response were either leading ($n = 34$) or lagging behind ($n = 22$) the changes in EEG-PR curve by more than 1.0 s. While the positively correlated samples more often showed a lag (6/7), the negatively correlated cases (33/51, $P = 0.005$) showed a lead. The temporal delay was variable, up to 30 s, but most often less than 15 s.

Oscillations

In addition to the unitary and gradual changes described above, we found much faster and periodic fluctuations in EEG-PR (ratio of low to high EEG frequencies) and single unit firing. These very frequently occurring, oscillatory changes had an almost stable cycle period in the range 4–10 s as deduced from the autocorrelation function (ACF) of the EEG-PR curve. Changes in the EEG-PR were in most cases accompanied by variations in the strength of dLGN light responses which showed the same or a reciprocal time course.

Thus, changes in both signals could be either positively or negatively correlated to each other (Figs 3 and 6). Because these changes usually occurred periodically, we could use the CCF to achieve a reliable quantification of the temporal relationship between variations in EEG-PR and spike rate.

In our simulated control tests ($n = 3000$), none of the ACFs of the stochastic signal had either a period (wavelength) larger than 3.5 s or an amplitude larger than $4.0 \times 10^{-3} \text{ s}^{-1}$. However, for almost all the EEG-PR curves measured the ACF period was larger than 3.5 s and even for the few exceptions (less than 1%), the ACF amplitude was at least close to the maximum obtained in simulated tests. Therefore, we did not set any individual criterion to distinguish significant from insignificant EEG-PR oscillations but applied the CCF analysis to the entire sample.

Table 2 gives an overview for the distribution of the strength of correlation (amplitude, |Amp|) between EEG-PR and overall spike rate and its relation to the period (wavelength) and correlation polarity of the oscillation. The statistics show that a smaller number of positively correlated cases occurs when the variations in EEG-PR and spike rate are strong (larger |Amp| values, especially when $|\text{Amp}| > 4.0 \times 10^{-3}$). This tendency is similar to but not as

significant as that for the slow gradations. The relation between |Amp| and mean wavelength is more pronounced, suggesting that stronger changes, and stronger correlations between EEG and spike rate, are on average associated with longer oscillation periods. No dependence could be found between |Amp| and temporal shift (phase difference) values.

According to the threshold settings by the simulated control tests, $\text{Amp} < -2.5 \times 10^{-3}$ indicates a significant negative correlation between variations in EEG-PR and spike rate, and $\text{Amp} > 2.5 \times 10^{-3}$ a positive correlation. Of the total of 3210 recordings 741 were found to reach this criterion and of these 367 cases were positively correlated. Although the oscillatory changes in EEG-PR occurred much more frequently than the slow gradations, the relative number of significantly correlated cases is much lower compared with the statistics on slow gradations (23.1 vs. 41.3%), and the number of positive correlations is considerably larger (49.5 vs. 23.7%).

The distributions of wavelength (oscillation period) and temporal shift for the 741 significant cases are shown in Fig. 5A and B, respectively. The wavelength values varied between 3.0 and 16.5 s, with 663 cases (89.5%) in the range 4.0–10.0 s. For the shift values the full range was –3.3 to

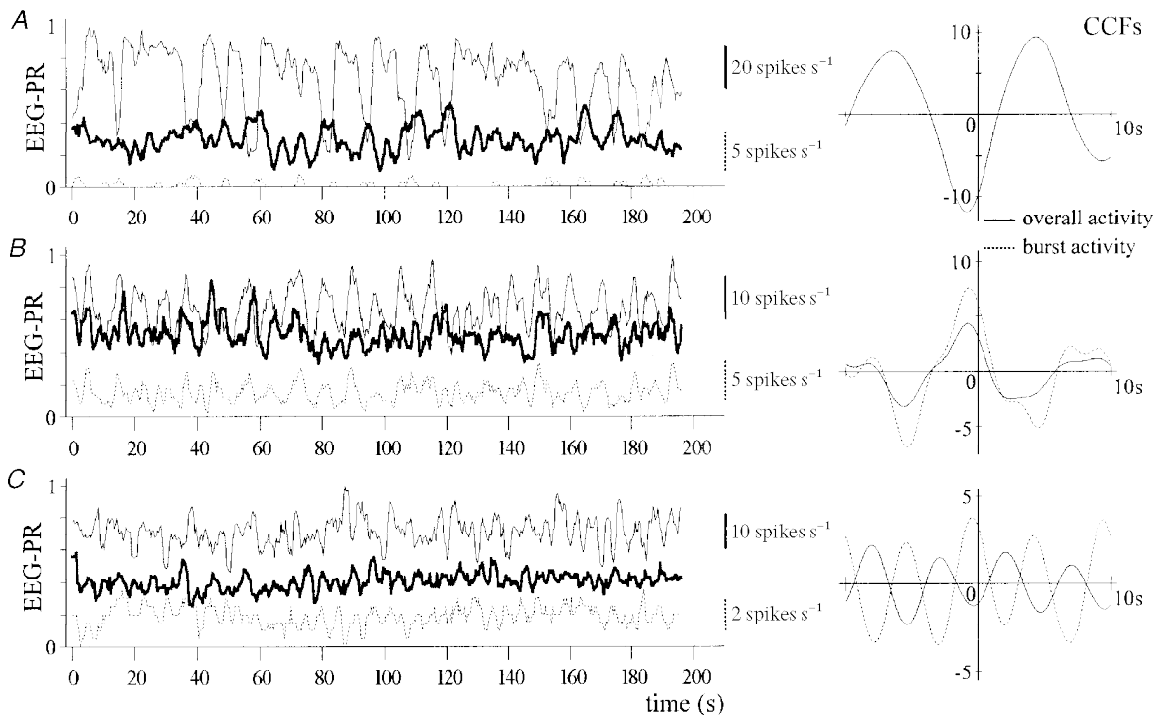


Figure 6. Examples for oscillatory events in EEG-PR (thick lines) and spike rate (thin lines)

In each panel (except A, right), the overall activity (thin continuous line) and burst activity (dashed line) of the same cell are shown to the left and, to the right, their CCFs to the EEG-PR. A, the overall activity displays a negatively correlated oscillation between spike rate and EEG-PR ($\text{Amp} = -20.516 \times 10^{-3}$). The burst firing is too weak to compute a CCF. B, the variations of both, overall activity and burst activity are positively correlated to the EEG-PR. $\text{Amp} = 7.176 \times 10^{-3}$ for overall activity; $\text{Amp} = 12.405 \times 10^{-3}$ for burst firing. C, the oscillatory changes are negatively correlated to the EEG for overall activity ($\text{Amp} = -2.872 \times 10^{-3}$), but positively correlated for burst firing ($\text{Amp} = 6.643 \times 10^{-3}$).

+2.8 s, with 572 cases (77.2%) within ± 1.0 s, indicating approximately synchronized variations in EEG-PR and visual responses.

Burst firing (dashed lines in Fig. 6) shows a slightly higher percentage of positive correlations (54.5% (925/1689) vs. 49.5% for overall activity, $P=0.025$), but a much larger proportion of general correlation (81.7% (1698/2079) vs. 23.1%), indicating a higher probability for oscillations to occur during burst firing. As during the slow gradations, the rate of burst activity changed in an opposite direction compared with the overall activity in many cases of oscillatory patterns (for example see Fig. 6C). We found 370

recordings with significant correlations of both overall activity and burst activity during oscillations of the EEG-PR. Of these, 175 cases (47.3%) showed anti-correlated changes in overall activity and burst activity.

Covariation in double-site recordings

The simultaneous recordings of the visual activity of two relay cells at different sites within the dLGN allowed an analysis of covariance of single unit activity with respect to the EEG. The analysis for slow gradations could be performed with 43 cell pairs which satisfied the condition that the changes in the EEG-PR and in the overall spike rate of each cell passed the threshold setting. Of the four

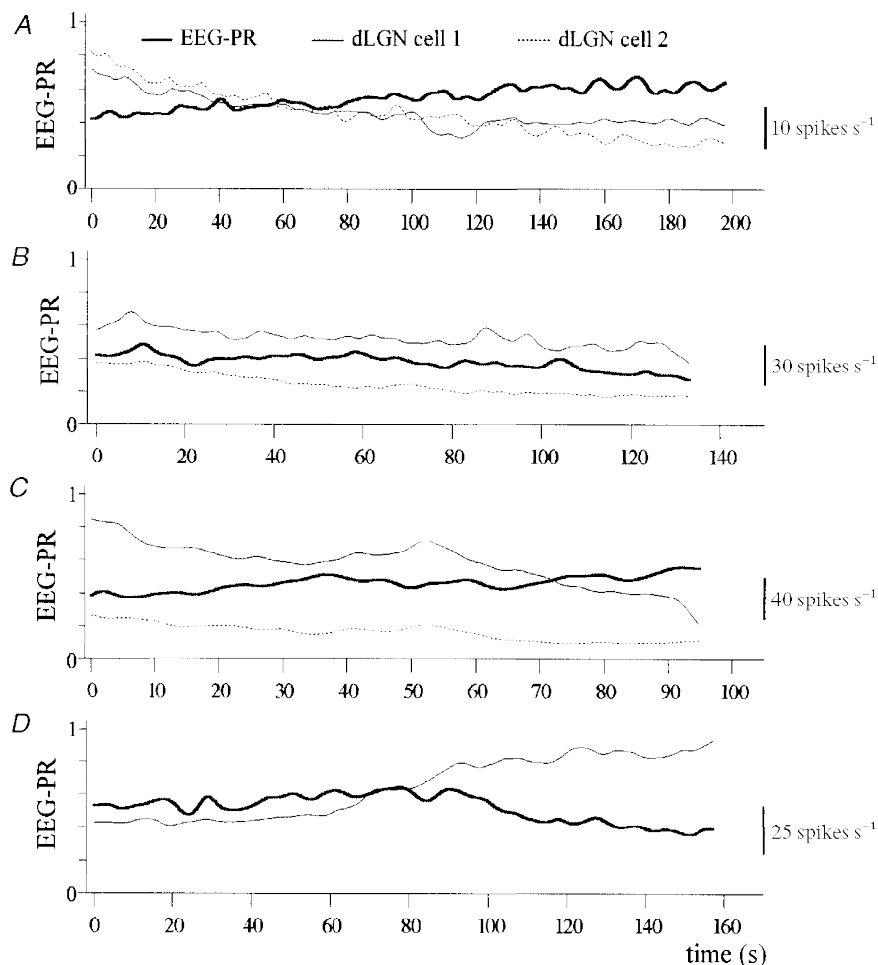


Figure 7. More examples of slow gradations in EEG-PR and spike rate, in this case for double-site recordings and variable correlation

In A–C, the overall responses of two simultaneously recorded cells are shown with thin continuous and dashed lines, respectively, and a common scale bar is used for both cells. All curves have been smoothed using filter a. Thick line, EEG-PR. A, both cells show a negatively correlated slow change in relation to the EEG-PR. $K_p = 1.060 \times 10^{-3} \text{ s}^{-1}$ and $K_s = -2.662 \times 10^{-3} \text{ spikes s}^{-1}$ for cell 1; $K_s = -5.143 \times 10^{-3} \text{ spikes s}^{-1}$ for cell 2. B, another recording from the same cell pair as shown in A, but recorded about 40 min later. Both cells reversed to a positive correlation, even though the change in cell 1 was insignificant. $K_p = -0.959 \times 10^{-3} \text{ s}^{-1}$ and $K_s = -2.045 \times 10^{-3} \text{ spikes s}^{-1}$ for cell 1; $K_s = -6.306 \times 10^{-3} \text{ spikes s}^{-1}$ for cell 2. C, still the same cell pair, recorded another 20 min later. Both cells returned to a negative correlation. $K_p = 1.349 \times 10^{-3} \text{ s}^{-1}$ and $K_s = -6.879 \times 10^{-3} \text{ spikes s}^{-1}$ for cell 1, $K_s = -9.556 \times 10^{-3} \text{ spikes s}^{-1}$ for cell 2. D, the slow gradation in spike rate is positively correlated to the EEG-PR during the first half of the single cell recording, but later on reversed to a negative correlation when the EEG-PR declined faster than it rose before.

possible combinations of the correlation polarities for the spike rates of 2 cells with the EEG-PR (2 even cases namely $+/+$ and $-/-$, and 2 odd cases $+/-$ and $-/+$) the overwhelming majority (41 pairs, 95.3%) was even (see Fig. 7A–C for examples), while only 2 pairs were odd. In the case of oscillatory events, 86 cell pairs were analysed in this way. Of these, 56 pairs were even (65.1%, see also Fig. 8A and C), but the other 30 pairs were odd (Fig. 8B). Even cases clearly dominated in oscillations (χ^2 test, $P < 0.02$), but their preponderance was not as strong as for the slow graduations. Furthermore, two simultaneously recorded cells usually tended to show a very close temporal relationship in their spike rate variations so resulting in a very small temporal shift between the maxima/minima of the CCF curves of the two cells (Fig. 8A and B). It should be noted that the receptive fields of the simultaneously recorded cells were well separated from each other, often by more than 10 deg. The high probability of covariation was therefore unlikely to have been due to common retinal inputs.

Relationship between slow graduations and oscillations

In many cases the fast fluctuations in EEG-PR and spike rate were around a relatively stable level for a long period (Fig. 6), but there were also examples in which the fast events were combined with slow graduations. We found combined slow and fast changes in EEG-PR in 52 of 741 recordings; a typical example is shown in Fig. 3. The χ^2 -test applied to the counts of the four possible combinations between the two correlation polarities (slow graduations/oscillations: $+/+$, $n = 2$; $+/-$, $n = 8$; $-/+$, $n = 19$; $-/-$, $n = 23$), could not reject the null hypothesis of independence ($P > 0.25$). In other words, no dependence could be found for the simultaneous appearance of oscillatory and steady gradual variations.

Variations in correlation

The correlation between variations in EEG-PR and spike rate was not stereotyped or invariable for the same dLGN relay cell throughout all recordings obtained from it. The

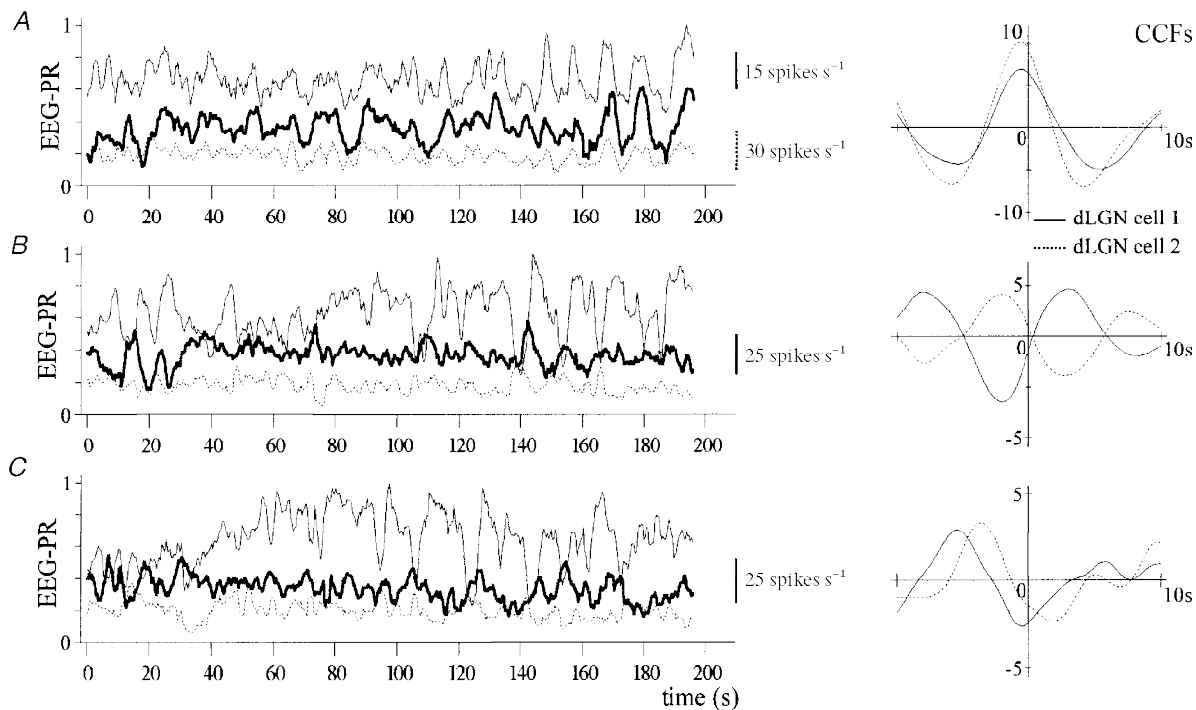


Figure 8. Further examples of oscillations in EEG-PR and spike rate, showing double-site recordings and variable correlation

In each panel, the overall responses of two simultaneously recorded cells, as well as their CCFs to EEG-PR, are shown with thin continuous and dashed lines, respectively. A common scale bar is used for both cells except in A. A, both cells show positively correlated oscillations, with spike rate changes leading. Values for cell 1 are: Amp = 11.459×10^{-3} , shift = -0.6 s, wavelength = 10.7 s; for cell 2: Amp = 16.997×10^{-3} , shift = -0.7 s, wavelength = 10.1 s. B, another recording on the same cell pair as shown in A, but recorded about 60 min later. Cell 1 reversed to a negative correlation with spike rate still leading (Amp = -10.999×10^{-3} , shift = -2.0 s, wavelength = 11.0 s), while the correlation for cell 2 became weaker but the temporal aspect changed very little (Amp = 7.438×10^{-3} , shift = -2.1 s, wavelength = 10.6 s). C, still the same cell pair recorded another 10 min later. For cell 1 the negative correlation became weaker (Amp = -4.633×10^{-3} , shift = -0.5 s, wavelength = 11.2 s), cell 2 also turned to a negative correlation, but spike rate changes now lagged behind (Amp = -4.163×10^{-3} , shift = 1.9 s, wavelength = 8.7 s). This case is, however, somewhat arguable, since it is also possible that the lead of cell 2 had increased to 3.6 s, but the correlation was still positive.

correlation amplitude or gradation slope, the temporal shift, and even the polarity (sign), could change among different recordings separated by a couple of minutes. This is the main reason why all statistics mentioned above are based on counts of recordings. Examples of variations in polarity can be seen in Fig. 7 for slow gradations and in Fig. 8 for oscillations. In some cases, reversal of correlation occurred even within 100 s, and were thus clearly visible in one recording (Fig. 7D). Qualitatively, the reversal of polarity in slow events often occurred along with changes in EEG-PR slope. However, the tendency of a certain cell for one polarity indicates that the polarity of correlation did not occur randomly.

Separate analyses for spontaneous activity, phasic and tonic responses

So far each correlation between dLGN relay cell firing and EEG was based on the overall spike rate, including all components of the visual response, and periods of more or less spontaneous activity. In a second step separate analyses of the kind described above were also performed for periods of spontaneous activity and for the phasic and tonic components of the visual responses. The results are as follows. (i) The variation of the tonic response is generally related to that of the overall activity which is not surprising, since overall activity is dominated by the number of spikes included in the tonic response component. In 91.8% of the slow gradations and in 80.4% of the oscillations the polarity of correlation was the same as for the overall activity. (ii) Spontaneous activity and phasic responses turn out to be different from the overall activity, with relatively fewer cases showing the same sign of correlation as for overall activity (64.9 and 48.5%, respectively, for slow gradations and 68.8 and 45.8%, respectively, for oscillations). (iii) The ratio of positive to negative correlations is very similar although, compared with the overall activity, the spontaneous activity shows slightly more positive correlations, whereas the tonic response behaves just the other way round.

DISCUSSION

General aspects

Previous studies have shown that in the anaesthetized cat the visual activity of dLGN relay cells during an activated EEG is quite different from that during a synchronized EEG (Livingstone & Hubel, 1981; Sawai *et al.* 1988; Funke & Eysel, 1992). A changing excitability and response mode of dLGN cells occurs in association with variations in the EEG pattern and may indicate state-dependent variations in information transmission efficiency along the primary visual pathway. The results from previous studies are like snapshots, showing distinct EEG patterns and the associated response modes. The intention of this study was to go a step further by (i) analysing the dynamics of the system and (ii) giving a more detailed quantitative description of the relationship between changes in the EEG pattern and changes in visually evoked activity in cat

dLGN. Both aspects were achieved by an almost continuous characterization of the spectral composition of the EEG and of the different response components of simultaneously recorded geniculate visual responses by the use of a sliding time-window analysis. In order to obtain a quantitative description of the EEG by a single parameter at any point in time, we calculated the ratio of the power of low (1–8 Hz) to high (20–40 Hz) frequency bands of the EEG (EEG-PR). This way we could demonstrate a very close relationship between the on-going global cortical activity (EEG) and the response characteristics of a single thalamic cell. Slow changes in the spectral composition of the EEG are reflected in changes in visual responses with very similar dynamics. Except for very slow and moderate changes, the increase in low-frequency power in the EEG is accompanied by a drop in tonic visual activity but an increase in the contribution of burst responses. Visual responsiveness can also follow rather fast, oscillatory changes of the EEG, usually within ± 1 s.

Changes on two different time scales: slow gradations and oscillations

With the use of the sliding time-window analysis we found two different patterns of variation in the spectral composition of the EEG that were correlated with changes in geniculate visual activity: (i) slow steady increments or decrements in the EEG-PR lasting up to minutes, termed 'slow gradations' and, (ii) fast, periodic changes within a few seconds which occurred in a repetitive manner for longer periods called 'oscillations'. These results were obtained from anaesthetized cats, but may also hold for a behaving animal since cats anaesthetized with nitrous oxide and halothane show spontaneous changes in EEG pattern (Ikeda & Wright, 1974; Livingstone & Hubel, 1981; Sawai *et al.* 1988; Funke & Eysel, 1992) which are comparable with changes of the EEG signal of the behaving cat (Lancel, 1993 and discussion below).

Slow gradations

In principle, our results concerning the slow gradations of EEG-PR confirm those results obtained in previous studies (Livingstone & Hubel, 1981; Sawai *et al.* 1988; Funke & Eysel, 1992), reflecting the different response modes of cat dLGN relay cells for very different EEG patterns (synchronized *vs.* non-synchronized or activated EEG). In the previous work, however, visual responses were averaged over 10–50 trials to represent the different global states. The present study was designed to analyse the dynamics and temporal relationships of this process and the chosen temporal resolution allows us to show correlations on the basis of single stimulus–response cycles. In this way we could demonstrate that a gradual change in the spectral composition of the EEG is also accompanied by gradual changes in the responsiveness of single dLGN relay cells. In general, the probability for a negative correlation between EEG-PR and response strength was greater, the stronger the change was. The tight coupling between the changes in single cell firing and the changes in overall activity, as reflected by the EEG, is demonstrated by the high

percentage (95.3%) of simultaneously recorded cell pairs showing correlated changes in spike rate.

Episodes with a changing EEG-PR were usually interspersed with periods of a rather stable state for several minutes. Similar variations have also been reported to occur during halothane–nitrous oxide anaesthesia (Ikeda & Wright, 1974; Sawai *et al.* 1988). These alternating patterns show a time course similar to that for the sleep–wake cycle of the behaving cat (Lancel, 1993) which appears to have a shorter period (about 30 min) and a higher repetition rate than in humans. The periodic or spontaneous alternations between different sleep stages, i.e. between weak (I and II) and deep (III and IV) sleep stages, offer the most likely explanation for the gradations of the EEG-PR. This sleep–wake cycle is well-known to be controlled primarily by the brainstem arousal system (for review see Hobson, 1989; McCormick, 1989, 1992; Steriade & McCarley, 1990; Steriade, 1991).

Oscillations

The oscillatory changes were characterized by relatively fast (usually every 4–10 s) oscillations in the EEG-PR (ratio of the power of low to high EEG frequencies), accompanied by phase-coupled changes in geniculate visual responsiveness. Because of the periodic pattern, the auto- and cross-correlation functions (ACF and CCF) were optimally suited for analysis of this process. Oscillatory variations of this kind seem to be very frequent because in 99% of the original EEG-PR curves the amplitude of the ACF exceeded the statistical amplitude maximum obtained in the simulated signals. This kind of activity pattern seems to be a widespread EEG phenomenon but it may not always be suprathreshold for detection by common analytical methods. In the case of cross-correlations between EEG-PR oscillations and oscillations of the dLGN spike rate 23.1% of the recordings exceeded the threshold set for significant correlations (2.5×10^{-3}), indicating that this rhythm is also a common phenomenon in thalamo-cortical processing. This rhythm was found in all experiments (15 animals) and, despite the general effect of anaesthesia, all cats were in a physiologically appropriate condition. Epileptiform activity was never observed. With a range of 3.0–16.5 s for all experiments the period (wavelength) of these oscillations was rather variable, although in most cases (about 90%) ranging within 4–10 s. The frequency of artificial ventilation partly overlaps with the range of the oscillatory frequencies but was always within a much smaller range (10–15 cycles min^{-1} or 4–6 s cycle^{-1}). For all those oscillations that exceeded the threshold determined by the simulation, the mean period length was 6.492 s and thus well outside the range of the respiratory cycle. As a direct control, in the final two experiments of this series, we made a protocol of the respiratory frequency throughout the experiment. The frequency was between 10 and 12 cycles min^{-1} (5–6 s cycle^{-1}) throughout each of the two experiments, but the dominating wave periods were found to be 10–12 s in one experiment and close to 8 s in the other.

Therefore, we can rule out the possibility that the oscillation of the EEG-PR is an artefact arising from artificial ventilation.

It is also unlikely that the oscillatory changes in the EEG are related to a vascular rhythm. Peripheral blood vessels undergo almost periodic changes of their vascular tone with a cycle length of 12–50 s (typically 25 s) which originates from membrane potential fluctuations of the smooth muscle cells (Siegel *et al.* 1980). An oscillation of similar cycle length (decaseconds) termed ‘cyclic alternating pattern’ (CAP) has been reported for EEG recordings obtained from human subjects during non-REM sleep (Terzano *et al.* 1988). CAPs were preferentially found during transitions from waking to sleep and during sleep recoveries after nocturnal awakenings, thus during phases of light sleep. This observation does conform with our results since oscillations of the spectral composition of the EEG (EEG-PR) occurred when δ waves were present but at the same time higher frequencies were not totally suppressed and dLGN relay cells showed tonic visual activity. The cycle length of CAPs and EEG-PR oscillations are not identical but it is possible that the process is faster in cats compared with humans just as the sleep cycle length is shorter in cats (see Lancel, 1993).

A more likely candidate for the origin of the periodic changes in the EEG-PR are the low-frequency oscillations (< 1 Hz) recently described by Steriade and coworkers in cat neocortical and thalamic electrical activity (Steriade *et al.* 1993*b,c*). This rhythm could be clearly separated from δ waves (1–4 Hz), but was in most cases accompanied by waxing and waning periods of δ activity or, in some cases associated with sleep spindles (7–14 Hz, Steriade *et al.* 1993*c*). It is possible that the slow rhythm reported by Steriade is homologous to the oscillatory fluctuations in EEG pattern observed by us. However, the frequency ranges are not exactly the same: 0.2–0.5 Hz for the slow rhythm (even higher during ketamine and nitrous oxide anaesthesia with 0.6–1 Hz, Steriade *et al.* 1993*b*), but 0.06–0.3 Hz for the oscillations we found. These differences in frequency may be related to the different anaesthetics used or to different anaesthetic levels. Steriade used urethane, ketamine – in part supplemented with nitrous oxide – or sodium pentobarbitone for anaesthesia, we used nitrous oxide supplemented with 0.4% halothane during recordings. We injected ketamine for surgery only during the initial episode of the experiment. Steriade has shown (1993*b*) that the frequency of the slow oscillation increased soon after injection of a small amount of ketamine (< 3–4 mg kg^{-1}) and discussed the possible involvement of NMDA-mediated postsynaptic processes. Another difference between Steriade’s and our studies is the visual stimulation used by us. We cannot exclude the possibility that a periodic afferent input may affect the oscillation frequency. On the other hand, we can exclude that the periodic stimulation is the primary reason for this slow oscillation because stimulus frequency (0.5 Hz) was different from oscillation frequency (0.06–0.3 Hz).

Steriade *et al.* (1993*b*) have shown that the slow rhythm occurs during natural sleep in cat and human and might, thus, be a property of slow wave (δ) sleep. On the other hand, we found the periodic variations in the EEG also during phases of vigorous tonic visual activity associated with relatively low δ activity, which are usually not related to deep sleep (Sawai *et al.* 1988; Funke & Eysel, 1992). Nevertheless, the present oscillations may be linked to the spontaneous slow oscillations described by Steriade since these oscillations are accompanied by periodical changes in the membrane potential of thalamic and cortical neurons. Both are hyperpolarized during a surface-negative EEG wave and may show an altered responsiveness to afferent inputs (Contreras *et al.* 1996). According to our results it is reasonable to suggest that this process is not limited to sleep but may take place also during the transmission mode.

So far, one can only speculate about the possible functions and origins of the short time scale variations in EEG. The slow rhythm (< 1 Hz) reported by Steriade *et al.* (1993*b*) survives extensive thalamic lesions (Steriade *et al.* 1993*c*), indicating a cortical origin. Our studies cannot be compared with those of Steriade directly because we analysed variations in visually driven activity while he investigated the temporal behaviour of intrinsically generated activity. It should be noted that we demonstrate, for the first time, relatively fast periodical changes in geniculate transmission and not changes in distinct thalamic firing patterns like the spindle or δ waves. Nevertheless, we also favour the origin of the modulatory control centre to be outside the principal thalamic sensory nuclei. In general, oscillatory EEG events of this kind seem to be too fast to be associated with changes in global arousal, but may reflect some characteristics of cortico-thalamic processing such as a recurrent flow control mechanisms via the corticofugal feedback system. The equal probability of positive and negative correlation and the variable temporal relationship indicate that the temporal phase of this oscillation is not identical throughout the dLGN. In other words, with respect to the information relayed, there seem to be multiple 'hot' as well as 'cold' spots in dLGN at any given time. In previous reports we have demonstrated that the temporal structure of the thalamic responses may influence signal transmission to the cortex on a fast (milliseconds) time scale (Funke & Wörgötter, 1995; Wörgötter & Funke, 1995; Funke *et al.* 1996; Wörgötter *et al.* 1998). The current findings additionally suggest that a flow-control from the thalamus to the cortex may exist also on a much slower time scale. The substrate for this internal control could be the cortico-thalamic feedback system.

The finding that oscillations of the EEG-PR and those of the spike rate of two simultaneously recorded dLGN relay cells could be positively correlated for one cell and negatively correlated for the other cell at the same time, is contrary to the opinion that cell activity is widely synchronized during the slow oscillation of the EEG (Steriade *et al.* 1993*b*). One explanation could be that

synchronization is not always perfectly in phase. During the development of synchronous activity cell assemblies might oscillate counter-sign for some time, an assumption which is thoroughly conceivable taking into account that a network of reciprocal excitatory and inhibitory connections has a tendency to develop such kinds of activity.

For the following reasons, we suggest that the slow gradations and oscillations of the EEG-PR and the correlated geniculate visual activity are reflections of two functionally different processes which are also controlled by independent neural mechanism. Slow gradations are dominated by negative correlations between EEG-PR and spike rate, and two simultaneously recorded dLGN relay cells show covariations of the visual activity with the same sign. The periodic variations of the EEG-PR seem to be either positively or negatively correlated to spike rate by chance, and covariations of two dLGN recordings were often counter-sign. In addition, the two patterns seem to occur independently of each other since different combinations of their correlation polarities were distributed almost randomly. Therefore, one could speculate that fast and slow events represent two different physiological processes.

Sign of correlation and temporal relationship between visual activity and EEG

Determination of the sign of correlation between the EEG-PR and the spike rate is quite exact for the slow variations. However, because of the modest slope of most of the slow variations the exact temporal relationship between the two signals was hardly measurable, in part because the onset of the change is not well defined or out of the range of one complete recording. Only the faster gradations which had a steeper slope and occasionally occurred within one recording allowed for an analysis of the temporal relations between EEG-PR and spike rate. The temporal delay between the change in both signals could be up to 30 s, but usually was only a few seconds. Changes in response strength could lead over or lag behind the changes in EEG. This result demonstrates that not all neurons in the dLGN change their response pattern exactly at the same time, pointing to a graded but still relatively fast change in activity throughout the population.

The role of burst firing

The separate analysis of burst firing during visual stimulation demonstrated that, contrary to the overall activity, burst firing was most often positively correlated (85.1%) to the EEG-PR during slow gradations. This finding is generally in accordance with previous results (Livingstone & Hubel, 1981; McCarley *et al.* 1983; Funke & Eysel, 1992). For the oscillatory events the proportion of positive and negative correlations was balanced, but the probability of positively correlated changes was considerably higher for burst activity than for overall activity. Thalamic relay cells show repetitive, spontaneous burst discharges when their cell membrane is hyperpolarized (Llinás &

Jahnsen, 1982). The enhancement of burst firing during an increased EEG-PR may be related to an increased probability of bursts occurring during the inhibitory phase of the stimulus cycle when the excitatory stimulus is switched off. In part, burst discharges can also occur at onset of a visual response when the cell is hyperpolarized (Lo *et al.* 1991; Lu *et al.* 1992) or the visual response is reduced to a short burst of activity when the EEG is dominated by δ waves (Sawai *et al.* 1988; Funke & Eysel, 1992). The fraction of visual responses started with a burst might increase and persist for some time while EEG synchronization proceeds. Due to their high signal-to-noise ratio bursts elicited by a sudden change in contrast may serve as a 'wake-up' call for the visual cortex and increase arousal (see Funke & Eysel, 1992; Guido & Weyand, 1995).

In summary, this study demonstrates that transmission of visual signals through the dLGN varies in correlation with changes in the spectral composition of the EEG. Transmission measured as spike rate is reduced during increased low-frequency activity (δ waves) and variation can be slow and steady or oscillatory with a tight locking to oscillations of the spectral composition of the EEG. Graded as well as periodic changes in dLGN transmission may be a reflection of arousal-related processes which may be global like the sleep-wake cycle or more restricted to spatial aspects within a sensory channel. Future studies are needed to clarify whether the slow gradual and somewhat faster oscillatory changes are expressions of different functional states.

- BASAR, E. (1980). *EEG-Brain Dynamics: Relation between EEG and Brain Evoked Potentials*. Elsevier/North-Holland Biomedical Press, Amsterdam, New York, Oxford.
- BULLIER, J. & NORTON, T. T. (1979). Comparison of receptive field properties of X and Y ganglion cells with X and Y lateral geniculate cells in the cat. *Journal of Neurophysiology* **42**, 274–291.
- CLELAND, B. G. & LEE, B. B. (1985). A comparison of visual responses of cat lateral geniculate nucleus neurones with those of ganglion cells afferent to them. *Journal of Physiology* **369**, 249–268.
- COENEN, A. M. L. & VENDRICK, A. J. H. (1972). Determination of the transfer ratio of cat's geniculate neurons through quasi-intracellular recordings and the relation with the level of alertness. *Experimental Brain Research* **14**, 227–242.
- CONTRERAS, D., TIMOFEEV, I. & STERIADE, M. (1996). Mechanisms of long-lasting hyperpolarizations underlying slow sleep oscillations in cat corticothalamic networks. *Journal of Physiology* **494**, 251–264.
- CURRO DOSSI, R., NUNEZ, A. & STERIADE, M. (1992). Electrophysiology of a slow (0.5–4 Hz) intrinsic oscillation of cat thalamocortical neurons *in vivo*. *Journal of Physiology* **447**, 215–234.
- DERRINGTON, A. M. & FUCHS, A. F. (1979). Spatial and temporal properties of X and Y cells in the cat lateral geniculate nucleus. *Journal of Physiology* **293**, 347–364.
- FUNKE, K. & EYSEL, U. T. (1992). EEG-dependent modulation of response dynamics of cat dLGN relay cells and the contribution of corticogeniculate feedback. *Brain Research* **573**, 217–227.
- FUNKE, K., NELLE, E., LI, B. & WÖRGÖTTER, F. (1996). Corticofugal feedback improves the timing of retino-geniculate signal transmission. *NeuroReport* **7**, 2130–2134.
- FUNKE, K., PAPE, H. C. & EYSEL, U. T. (1993). Noradrenergic modulation of retinogeniculate transmission in the cat. *Journal of Physiology* **463**, 169–191.
- FUNKE, K. & WÖRGÖTTER, F. (1995). Temporal structure in the light response dynamics of relay cells in the dorsal lateral geniculate nucleus of the cat. *Journal of Physiology* **485**, 715–737.
- GUIDO, W. & WEYAND, T. (1995). Burst responses in thalamic relay cells of the awake behaving cat. *Journal of Neurophysiology* **74**, 1782–1786.
- HIRSCH, J. C., FOURMENT, A. & MARC, M. E. (1983). Sleep-related variations of membrane potential in the lateral geniculate body relay neurons of the cat. *Brain Research* **259**, 308–312.
- HOBSON, J. A. (1989). *Sleep*. Scientific American Library, New York.
- IKEDA, H. & WRIGHT, M. J. (1974). Sensitivity of neurons in visual cortex (area 17) under different levels of anaesthesia. *Experimental Brain Research* **20**, 471–484.
- LANCEL, M. (1993). Cortical and subcortical EEG in relation to sleep-wake behaviour in mammalian species. *Neuropsychobiology* **28**, 154–159.
- LANCEL, M., VAN RIESEN, H. & GLATT, A. (1992). The time course of sigma activity and slow-wave activity during NREMS in cortical and thalamic EEG of the cat during baseline and after 12 h of wakefulness. *Brain Research* **596**, 285–295.
- LINDSLEY, D. B. & WICKE, J. D. (1974). The electroencephalogram: autonomous electrical activity in man and animals. In *Bioelectric Recording Techniques*, part B, *Electroencephalography and Human Brain Potentials*, ed. THOMSON, R. F. & PATTERSON, M. M. pp. 3–83. Academic Press, New York.
- LIVINGSTONE, M. S. & HUBEL, D. H. (1981). Effects of sleep and arousal on the processing of visual information in the cat. *Nature* **291**, 554–561.
- LLINÁS, R. & JAHNSEN, H. (1982). Electrophysiology of mammalian thalamic neurons *in vitro*. *Nature* **297**, 406–408.
- LO, F. S., LU, S. M. & SHERMAN, S. M. (1991). Intracellular and extracellular *in vivo* recording of different response modes for relay cells of the cats lateral geniculate nucleus. *Experimental Brain Research* **83**, 317–328.
- LU, S. M., GUIDO, W. & SHERMAN, S. M. (1992). Effects of membrane voltage on receptive field properties of lateral geniculate neurons in the cat – contributions of the low-threshold Ca²⁺ conductance. *Journal of Neurophysiology* **68**, 2185–2198.
- MCCARLEY, R. W., BENOIT, O. & BARRIONUEVO, G. (1983). Lateral geniculate nucleus unitary discharge in sleep and waking: State- and rate-specific aspects. *Journal of Neurophysiology* **50**, 798–818.
- MCCORMICK, D. A. (1989). Cholinergic and noradrenergic modulation of thalamocortical processing. *Trends in Neurosciences* **12**, 215–221.
- MCCORMICK, D. A. (1992). Cellular mechanisms underlying cholinergic and noradrenergic modulation of neuronal firing mode in cat and guinea pig dorsal lateral geniculate nucleus. *Journal of Neuroscience* **12**, 278–289.
- MCCORMICK, D. A. & PAPE, H. C. (1990). Properties of a hyperpolarization-activated cation current and its role in rhythmic oscillations in thalamic relay neurons. *Journal of Physiology* **431**, 291–318.
- PRESS, W. H., FLANNERY, B. P., TEUKOLSLEY, S. A. & VETTERLING, W. T. (1988). *Numerical Recipes in C: The Art of Scientific Computing*. Cambridge University Press, Cambridge, New York, Melbourne.

- SAWAI, H., MORIGIWA, K. & FUKUDA, Y. (1988). Effects of EEG synchronisation on visual responses of cat's geniculate relay cells: a comparison among Y, X and W cells. *Brain Research* **455**, 394–400.
- SIEGEL, G., EBELING, B. J. & HOFER, H. W. (1980). Foundations of vascular rhythm. *Berichte der Bunsengesellschaft für Physikalische Chemie* **84**, 403–406.
- SINGER, W. (1977). Control of thalamic transmission by corticofugal and ascending reticular pathways in the visual system. *Physiological Reviews* **57**, 386–420.
- SINGER, W., TRETTER, F. & CYNADER, M. (1976). The effect of reticular stimulation on spontaneous and evoked activity in the cat visual cortex. *Brain Research* **102**, 71–90.
- STERIADE, M. (1991). Alertness, quiet sleep, dreaming. In *Cerebral Cortex*, vol. 9, ed. PETERS, A. & JONES, E. G., pp.279–357. Plenum Press, New York, London.
- STERIADE, M. & MCCARLEY, R. W. (1990). *Brainstem Control of Wakefulness and Sleep*. Plenum Press, New York, London.
- STERIADE, M., MCCORMICK, D. A. & SEJNOWSKI, T. J. (1993a). Thalamocortical oscillations in the sleeping and aroused brain. *Science* **262**, 679–685.
- STERIADE, M., NÚÑEZ, A. & AMZICA, F. (1993b). A novel slow (< 1 Hz) oscillation of neocortical neurons *in vivo*: depolarising and hyperpolarising components. *Journal of Neuroscience* **13**, 3252–3265.
- STERIADE, M., NÚÑEZ, A. & AMZICA, F. (1993c). Intracellular analysis of relations between the slow (< 1 Hz) neocortical oscillation and other sleep rhythms of the electroencephalogram. *Journal of Neuroscience* **13**, 3266–3283.
- STONE, J. & HOFFMANN, K. P. (1971). Conduction velocity as a parameter in the organisation of the afferent relay in the cat's lateral geniculate nucleus. *Brain Research* **32**, 454–459.
- TERZANO, M. G., PARRINO, L. & SPAGGIARI, M. C. (1988). The cyclic alternating sequences in the dynamic organization of sleep. *Electroencephalography and Clinical Neurophysiology* **69**, 437–447.
- WÖRGÖTTER, F. & FUNKE, K. (1995). Fine structure analysis of temporal patterns in the light response of cells in the lateral geniculate nucleus of cat. *Visual Neuroscience* **12**, 469–484.
- WÖRGÖTTER, F., NELLE, E., LI, B. & FUNKE, K. (1998). The influence of the corticofugal feedback on the temporal structure of visual responses of cat dorsal lateral geniculate relay cells. *Journal of Physiology* **509**, 797–815.

Acknowledgements

The authors are grateful for the technical support of B. Bendmann, P. Hendrich and V. Onasch. We also gratefully acknowledge the help of D. Ballantyne for improving the style of the manuscript. This study was supported by the Deutsche Forschungsgemeinschaft (Wo 388/4-2,3; Ey 8/21) and by the National Natural Science Foundation of China (NNSFC).

Corresponding author

K. Funke: Abteilung Neurophysiologie, Ruhr-Universität Bochum, Universitätsstraße 150, 44780 Bochum, Germany.

Email: funke@neurop.ruhr-uni-bochum.de